Observations from the ASPERA-3 ELS of Photoelectrons in the Tail of MARS

Frahm, R. A., J. D. Winningham, J. R. Sharber *(Southwest Research Institute, San Antonio, Texas)*

D. R. Linder, A. J. Coates *(Mullard Space Science Laboratory, Univ. College London, United Kingdom)* **and ASPERA-3 Team** *(Swedish Institute of Space Physics, Kiruna, Sweden)*

Abstract

The Analyzer of Space Plasma and Energetic Atoms (ASPERA-3) experiment is currently sampling plasma in the vicinity of Mars. ASPERA-3 determines the electron, ion, and neutral particle components of the plasma using four instruments: Electron Spectrometer (ELS), Ion Mass Analyzer (IMA), Neutral Particle Imager (NPI), and Neutral Particle Detector (NPD). The ELS instrument measures 128 logarithmically spaced samples of the electron spectrum between 1 eV and 20 keV every four seconds. Its eight percent energy resolution is used to resolve the carbon dioxide photoelectron peaks which are a dominant feature in the Martian Ionosphere. These same photoelectron signatures from carbon dioxide are also detected at distance greater than 1000 km in the Martian tail, providing experimental observation of electron escape from Mars. Implications of atmospheric escape will be discussed on these findings.

Introduction

The European Space Agency (ESA) Mars Express spacecraft (launched June 2, 2003) reached Mars and was injected into orbit on December 25, 2003. One of the Mars Express experiments is the Analyzer of Space Plasmas and Energetic Atoms-3 (ASPERA-3) [Barabash, et al., 2000, 2004] which has been measuring ions, electrons, and energetic neutral atoms (ENAs) at Mars. The Electron Spectrometer (ELS) is the instrument of the ASPERA-3 experiment.

Prior to launch of the Mars Express spacecraft, it was known that the ionospheric spectrum contained photoelectron peaks from the atmospheric gasses, measured most recently by Mars Global Surveyor (MGS) Electron Reflectometer (ER) [Mitchell et al., 2001]. The major photoelectron peaks in the range of 21-24 eV and 27 eV result from CO_2 ionization by a solar He 304 Å photon [Mantas and Hanson, 1979; Fox and Dalgarno, 1979]. The ELS was designed to measure these photoelectron peaks using its high-resolution modes to probe the high-altitude ionosphere and obtain a spectrum of the major photoelectron peaks. ELS is the first high-resolution ($\Delta E/E = 8\%$) electron spectrometer to observe the electron plasma in the region of a planet other than Earth.

Instrument

The ELS is a spherical tophat which samples electrons from a 4° high plane, divided into 16 sectors, each sector is 22.5° wide. ELS k-factor (7.23 ± 0.05 eV/volt) and resolution (0.083 ± 0.003 $\Delta E/E$) are slightly sector dependent and were determined by laboratory measurements at 10 keV. Energy deviations of the k-factor and resolution were folded into an energy-dependent relative microchannel plate (MCP) efficiency factor. This allowed determination of the energy independent physical geometric factor as 5.88×10^{-4} cm^2 sr.

ELS covers the energy range from 1 eV to 20 keV with two deflection power supplies. ELS deflection voltage ranges from 0 to 20.99 V for the low range and 0 to 2800.0 V for the high range (energy conversion is sector dependent, but approximately 150 eV and 20 keV for the max values). Each supply has a control resolution of 4096 linear voltage values within its full range. Of the 8192 possible deflection voltage values, 128 are selected to comprise the ELS energy sweep which occurs in 4 sec.

ELS Data

Three cases of ELS data are shown to illustrate atmospheric photoelectrons. Case 1: May 9, 2004 (day 130), in which the spacecraft is in the ionosphere at an altitude of 300 km. Case 2: June 14, 2004 (day 166), in which the spacecraft is in the tail at an altitude of 4000 km. Case 3: April 24, 2004 (day 115), in which the spacecraft is in the tail at an altitude of 7000 km.

Case 1: May 9, 2004 (Day 130)

When Mars Express is on the planet's dayside in the ionosphere, it detects atmospheric photoelectrons. The highest concentration of CO^2 is at the exobase of the planet, at about 100 km altitude. An example of observations of atmospheric photoelectrons at 300 km altitude is shown by the ELS data taken on May 9, 2004 (day 130) in Figure 1. Figure 1 shows an energy-time spectrogram for ELS sectors 0, 3, 6, 9, 12, and 15 with an enhanced energy intensity (EI) color scale to elucidate the atmospheric photoelectrons. Atmospheric photoelectrons are observed at all mounting angles through out the ELS sensor plane. ELS sectors 0, 12, and 15 view over the spacecraft and detect electrons emitting from its surface mixed with those of atmospheric/ionospheric origin. Figure 1 indicates that the atmospheric photoelectrons are observed at all mounting angles.

Figure 2 shows the 3 minute averaged energy intensity spectrum for ELS sector 3, 6, 9, and 12. A screen protection grid in ELS blocks high fluxes of electrons with energies less than 5 eV from detection at this time. The atmospheric photoelectron peaks are seen as a distinct enhancement in the electron spectrum. Theory predicts that the larger energy peak should occur at 27 eV. Using this value as fact, observations of spacecraft charging levels for this case are about -5 volts.

A contour of these ELS spectra is shown in Figure 3 for all ELS sectors and reveals the uniformity of the averaged features. The Atmospheric photoelectron peak is cleanly observed in all sectors. At energies below the photoelectrons, spacecraft secondary emission dominates the contour (the spacecraft is located in the upper left quadrant of this figure).

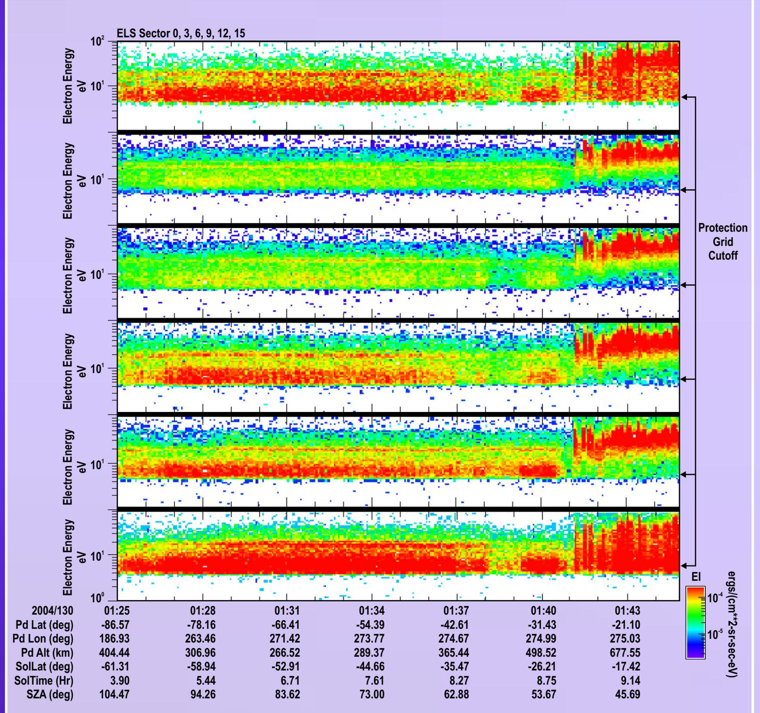

Figure 1. Energy-time spectrograms from May 9, 2004 (Day 130) showing enhanced energy intensity of atmospheric photoelectrons.

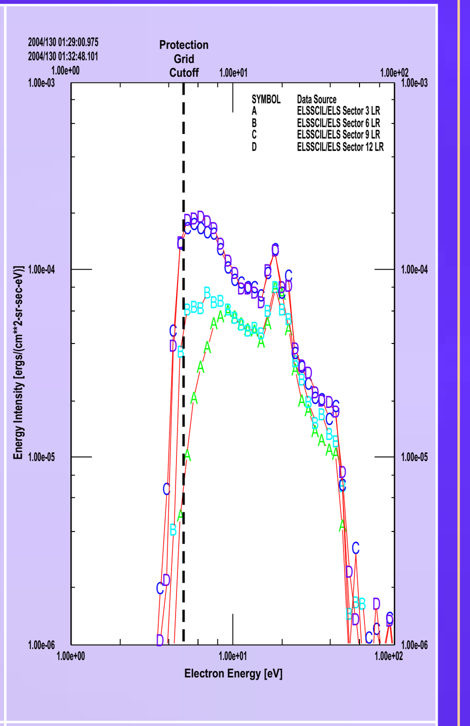

Figure 2. Averaged electron spectra from Figure 1 showing Co_2 ionization peaks. These data indicate that the spacecraft is charged by -5 volts at this time.

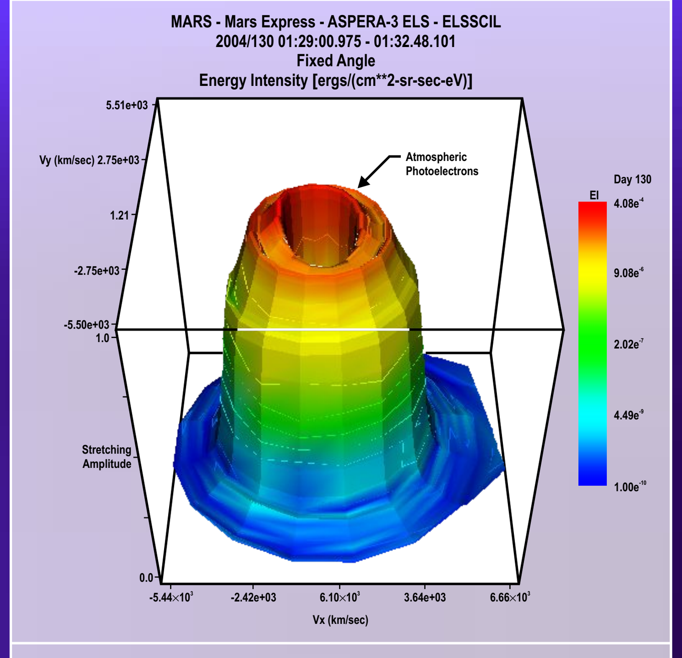

Figure 3. A contour of ELS data from the May 9, 2004 showing atmospheric photoelectrons are observed at all mounting angles and the angular extent of secondary electrons emitted from the spacecraft.

Case 2: June 14, 2004 (day 166)

Mars Express is in the planet's northern hemisphere dawnside as it travels from the sheath and into the Martian tail on June 14, 2004 (day 166). Electron data is measured from activation at about 18:00 UT in the sheath through the Martian tail between about 19:50 UT to 20:07 UT. Between sheath and tail plasma, atmospheric photoelectrons shown in Figure 4 are observed. Data in Figure 4 are presented in energy-time spectrogram format for ELS sectors 1, 2, 3, 4, 5, and 6 with an enhanced energy intensity color scale to elucidate the atmospheric photoelectrons. The ELS observed photoelectrons show an angular dependency as there is less photoelectron intensity in sectors 1 and 6 than in sectors 2, 3, 4, and 5. The most intense photoelectrons are observed in sectors 3 and 4 rather than in 2 and 5, particularly at the lower altitude edge of the data.

Electron spectra indicate that the spacecraft is charged positively in the sheath to +10 volts. At about 19:10 UT, the spacecraft charge begins to change to a negative potential and by 19:20 UT, the charge on the spacecraft is negative and atmospheric photoelectrons appear. The atmospheric photoelectrons have roughly the same energy until about 19:28 UT and this indicates that the charge developed on the spacecraft is steady.

Figure 5 shows 7.5 minute averaged energy intensity spectra for ELS sector 3, and 14 at two times. The screen protection grid in ELS is set to zero volts. The spectra at the left are taken from the time atmospheric photoelectrons are visible. Sector 3 shows CO_2 photoionization peaks. It views away from the spacecraft and toward the planet. Since theory predicts that the higher-enegy peak should occur at 27 eV, the spacecraft charging level derived from theory is about -7 volts. Sector 14 views across the spacecraft and detects a mixture of spacecraft generated electrons and electrons from the environment. Spacecraft generated electrons are detected at the energy of escape; this is not the case for electrons from the environment which are influenced by the spacecraft charge.

The spectra at the right are obtained from the sheath. Like the spectra on the left, the sun is about 0.75° from the ELS detection plane. An averaged spectrum is shown for each sector. In the sheath, the positive spacecraft potential is seen in the spectra of both ELS sectors. Since the electron plasma in the sheath is more energetic, the photoelectron peak produced from the spacecraft is resolved. One notes that since these electrons are generated at the spacecraft, they are detected at the spacecraft with their ionization energy, no matter if the spacecraft is positively or negatively charged.

A contour of the ELS spectra from the photoelectron region is shown in Figure 6 for all ELS sectors. Figure 6 reveals that the atmospheric photoelectron peaks are observed cleanly in the space-viewing sensors while photoelectrons from the spacecraft and spacecraft generated secondary electrons dominate the in sensors which look across the spacecraft.

Case 3: April 24, 2004 (day 115)

Mars Express is approximately at the equator on the planet's duskside. Shown in Figure 7 is the observed electron energy intensity for April 24, 2004 (day 115) energy-time spectrograms from ELS sectors 1 through 6. Atmospheric photoelectrons are encountered in sectors 1, 2, and 3 at 7100 km altitude first. Then, at about 6750 km altitude, atmospheric photoelectrons are encountered in sectors 1 through 6.

Figure 8 shows the predicted orbit location in cylindrical coordinates where the viewing directions of sectors 1 through 6 and sector 10 are shown. This plot confirms that sectors 1 through 6 view plasma coming from the direction of the planet and sector 10 views plasma coming from the planet's tail. As a reminder, sector 10 views free space and is not blocked by the spacecraft. The sun is below the ELS detection plane by about 1°.

Figure 9 shows 3 minute averaged energy intensity spectra for ELS sector 2 (view toward planet) and 10 (view toward tail) at the time when the photoelectrons are first encountered. The screen protection grid in ELS is set to -5 volts at this time. The spectra from both sectors show atmospheric electrons are visible. At energies greater than the atmospheric photoelectron peaks, both spectra show comparable levels of energy intensity. Within the atmospheric photoelectron peaks, there is a hint that those returning from the tail have been degraded and are beginning to cascade to slightly lower energies. Since theory predicts that the higher-energy CO_2 peak should occur at 27 eV, the spacecraft charging level derived from theory is about -10 volts (sector 2 peaks have been used). For energies lower than the atmospheric photoelectron peaks, there is more energy intensity (and therefore more electrons carring that energy) returning from the tail than headed into the tail.

A Contour of the ELS spectra from the photoelectron region of Figure 9 is shown in Figure 10 for all ELS sectors. The location of sectors 2, 6, and 10 are marked for orientation. Peaks of atmospheric photoelectrons can be seen in the contour, both at the position of sector 2 and at sector 10.

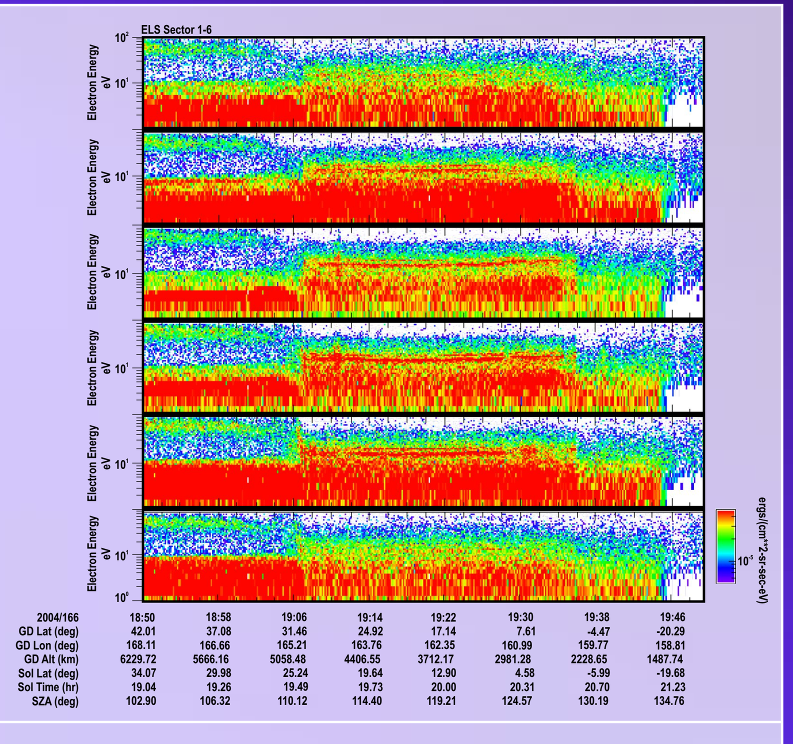

Figure 4. Energy-time spectrograms from June 14, 2004 (day 166) show enhanced energy intensity of atmospheric photoelectrons between 2000 and 5000 km altitude from the planet.

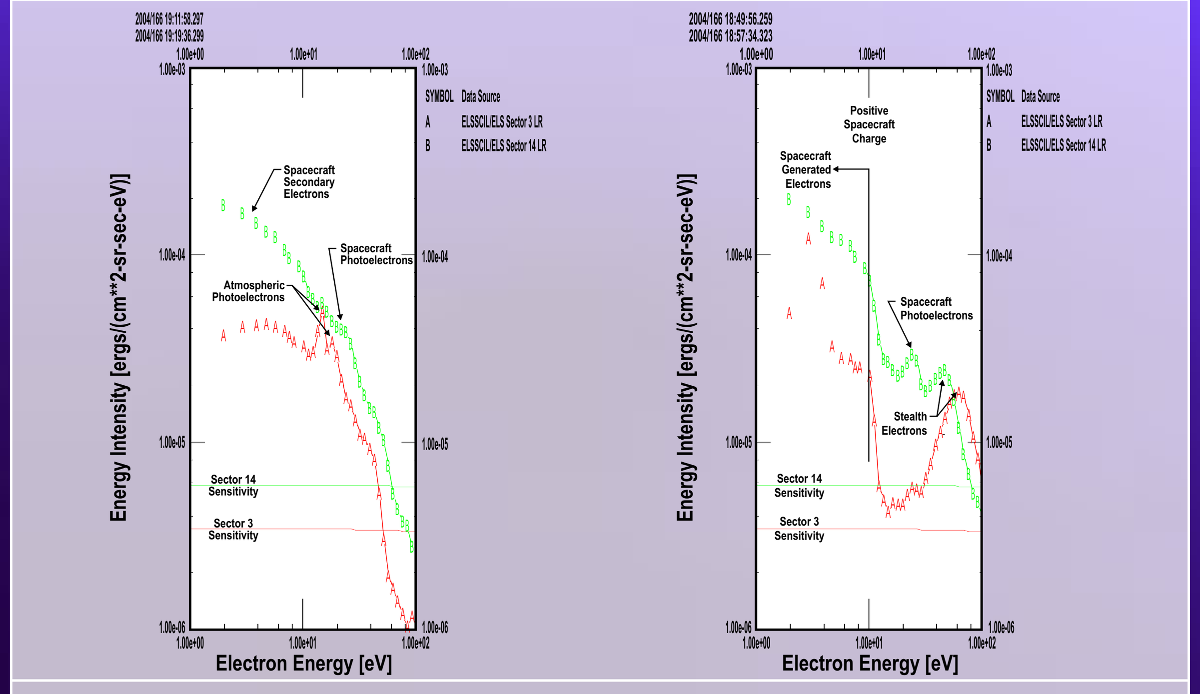

Figure 5. Averaged electron spectra from Figure 4 showing CO_2 ionization peaks at the left, suggesting a spacecraft charge of -7 volts, and from the sheath region at the right where the spacecraft charge is +10 volts.

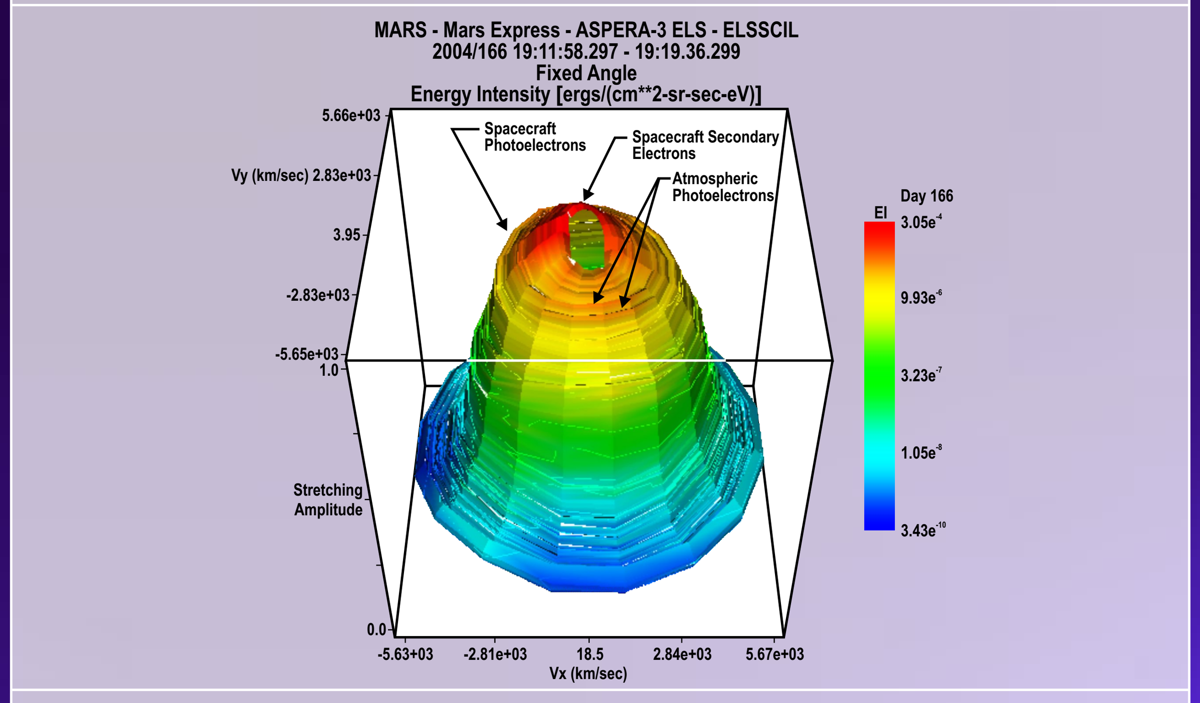

Figure 6. A contour of ELS data from June 14, 2004 showing atmospheric photoelectrons. Atmospheric photoelectrons are observed only when viewing away from the spacecraft and spacecraft photoelectrons dominate when viewing across the spacecraft.

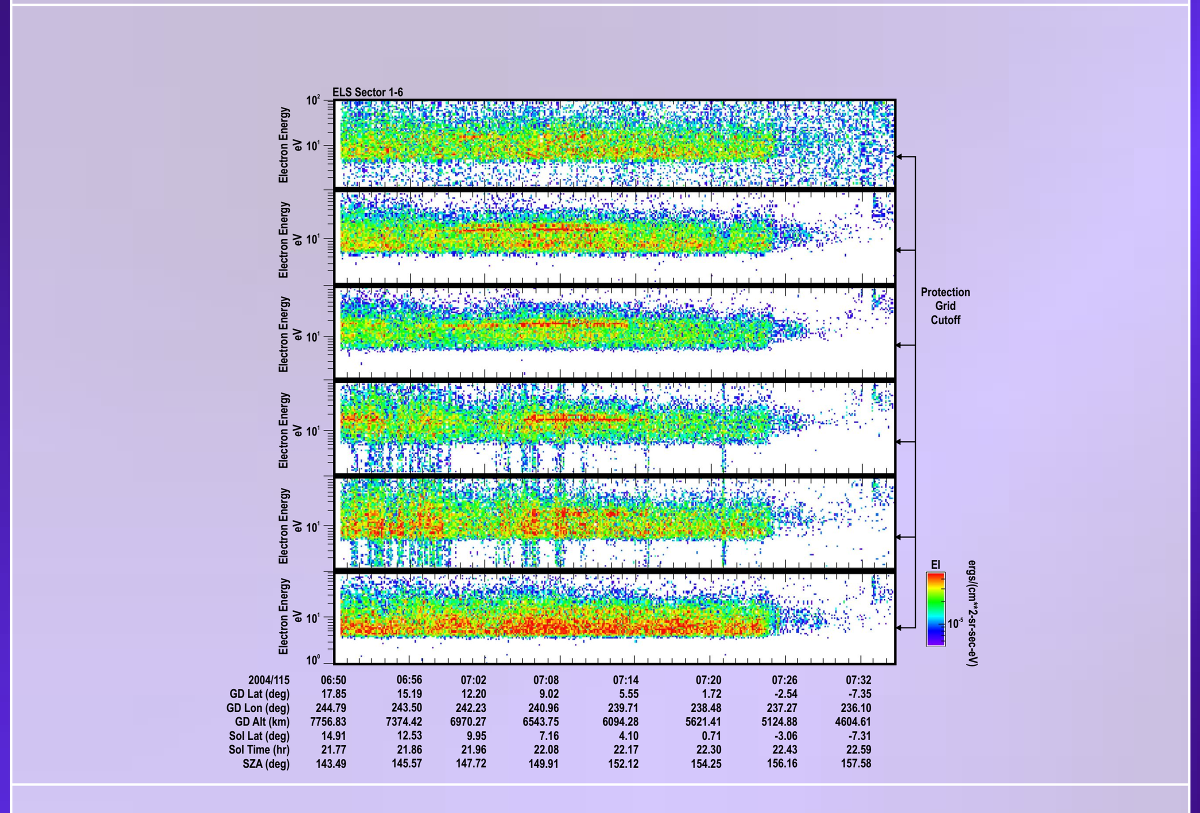

Figure 7. Energy-time spectrograms from June 14, 2004 (day 166) show enhanced energy intensity of atmospheric photoelectrons between 2000 and 5000 km altitude from the planet.

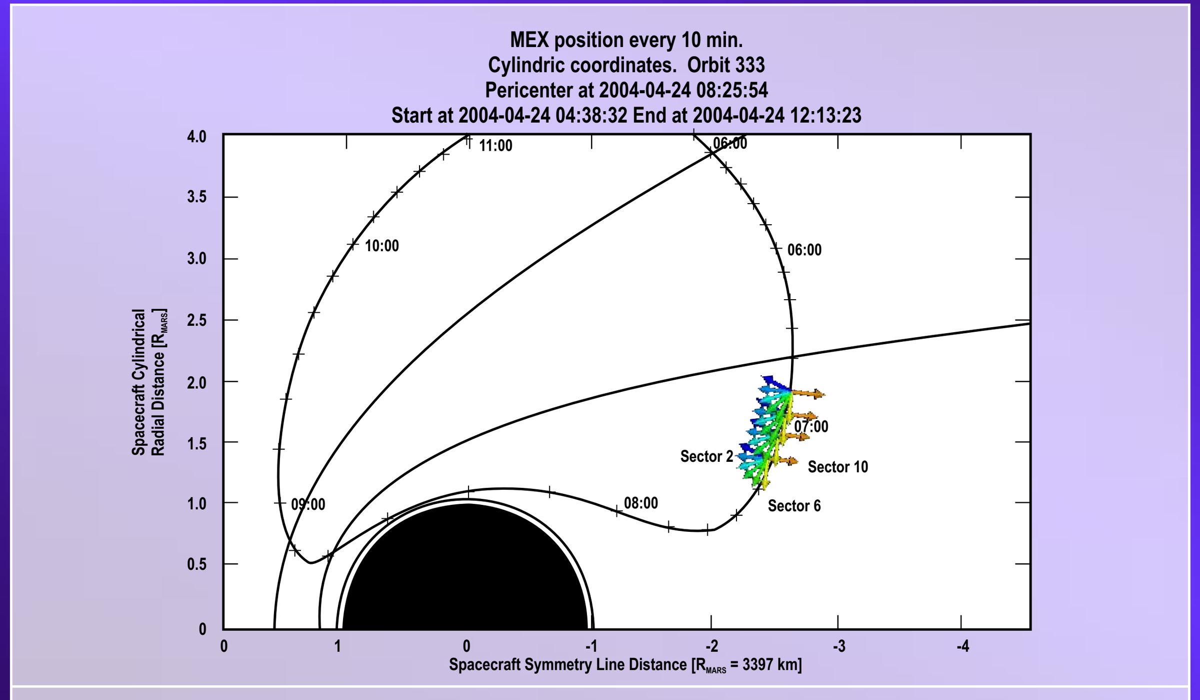

Figure 8. The predicted orbit of the Mars Express spacecraft has highlighted the region of space where atmospheric photoelectrons are observed with arrows indicating ELS viewing directions. These are indicated at the 10 minute markers of ELS.

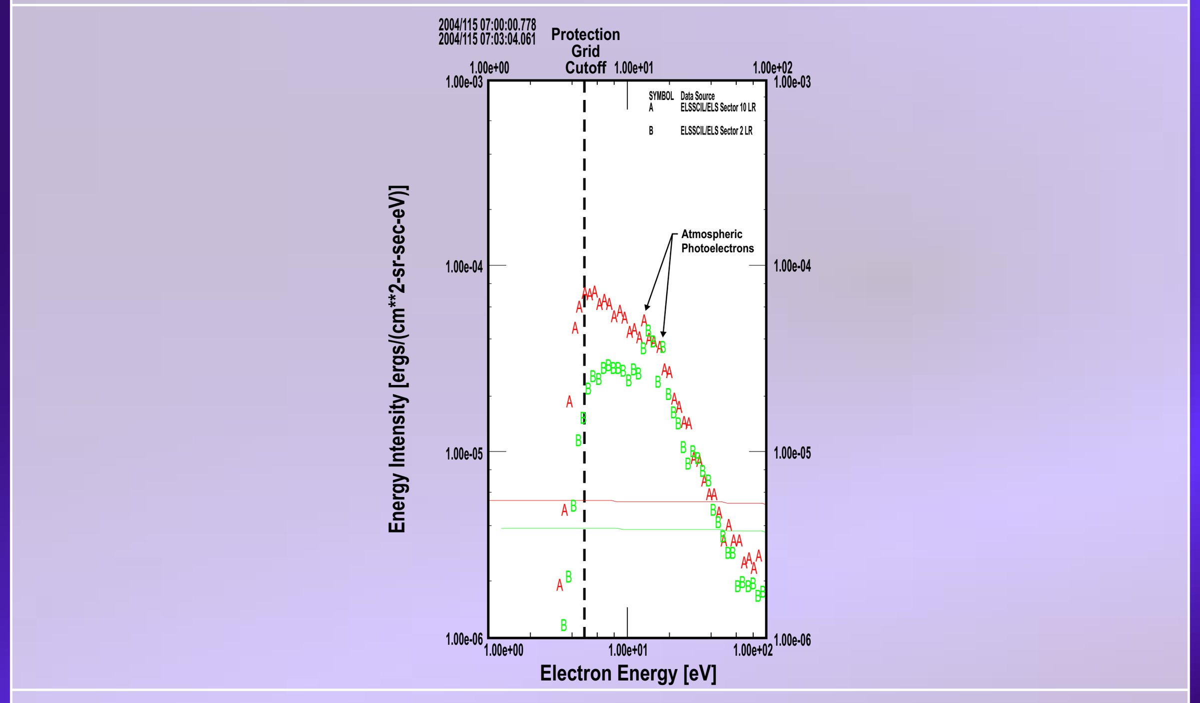

Figure 9. Averaged electron spectra from Figure 7 showing CO_2 ionization peaks in both the sector 2 viewing toward the planet and sector 10 viewing toward the planet's tail. Sector 2 spectra suggest a spacecraft charge of -10 volts.

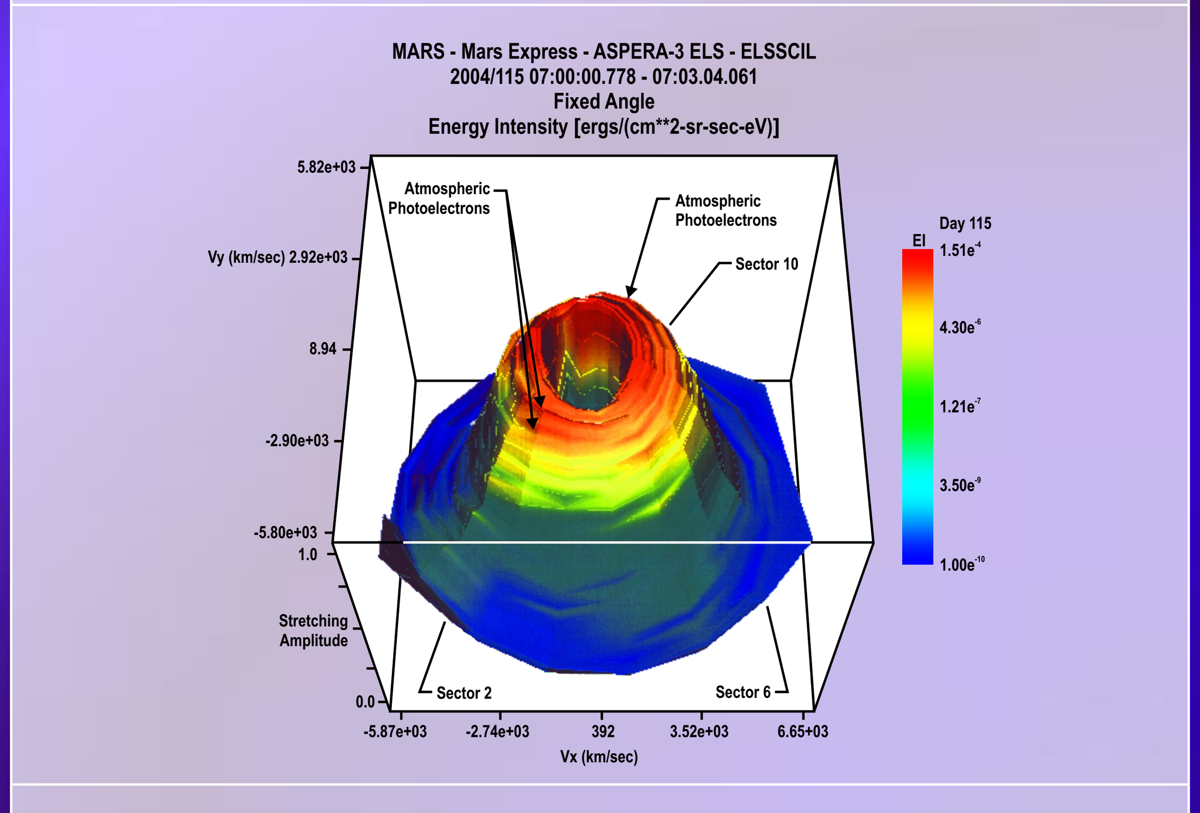

Figure 10. A contour of ELS data from April 24, 2004 (day 115) showing atmospheric photoelectrons are flowing both away and toward the planet.

Discussion

Spectra like case 1 are observed at almost all times while in the sunlit ionosphere. Their disappearance is typically related to a magnetic anomaly. For atmospheric photoelectrons observed in the tail, case 2 is typical. Atmospheric photoelectrons are observed escaping the planet, but no clear statement can be made about whether or not atmospheric photoelectrons are returning from the tail. Thus, for the majority of cases, ELS definitely observes atmospheric photoelectrons generated at the exobase of the planet, escaping down the tail from the planet along the sheath boundary.

To date, case 3 is the only data set obtained where atmospheric photoelectrons are observed by ELS sectors viewing toward and away from the planet simultaneously. This observation seems to indicate that atmospheric photoelectrons are counter streaming along the sheath boundary. The added intensity of electrons at energies below the atmospheric photoelectrons from plasma returning from the tail and the lack of plasma intensity difference above the atmospheric photoelectrons when comparing the forward and aft spectrum suggest that there has been an additional source of low-energy electrons added to the returning electron population.

Conclusion

The ELS instrument measures atmospheric photoelectrons at Mars. When detecting atmospheric photoelectrons, a high enough plasma density exists to drive the spacecraft potential negative, up to about -10 volts. Spacecraft potentials observed in the sheath are positive to +10 volts. Spacecraft charging levels observed in the tail when atmospheric photoelectrons are present and in the ionosphere are similar.

The spacecraft emits both photoelectrons and secondary electrons which produce a signal which can dominate that from the environment. Spacecraft photoelectron emission is dependent on the angle at which the sun strikes the spacecraft surface over which ELS measures.

Atmospheric photoelectrons dominate the ionospheric photoelectron spectrum and are observed almost all of the time. Their detection in sensors viewing across the spacecraft are dependent on the intensity levels of spacecraft electrons.

At least one deep tail measurement of atmospheric photoelectrons is in shadow enough to measure returning atmospheric photoelectrons from the tail. Both atmospheric photoelectrons escaping from the planet and those returning show higher intensity than the adjacent photoelectrons in the energy spectrum; although the returning atmospheric photoelectrons show some degradation in energy location indicating that they are cascading. Electrons at energies lower than the CO_2 peaks are observed with higher intensity returning from the tail than leaving the planet, possibly indicating that a source is adding low energy plasma to the region.

Acknowledgements

The ASPERA-3 experiment on the European Space Agency (ESA) Mars Express mission is a joint effort between 15 laboratories in 10 countries, all sponsored by their national agencies. We thank all these agencies as well as the various departments/institutes hosting these efforts. We wish to acknowledge support through the National Aeronautics and Space Administration (NASA) contract NASW-00003 in the United States, Particle Physics and Astronomy Research Council (PPARC) in the United Kingdom, and wish to thank those NASA officials who had the foresight to allow augmentation of the original ASPERA-3 proposal for ELS so that it would provide the additional capabilities which allowed the science described in this paper to be conducted. We also wish to acknowledge the Swedish National Space Board for their support of the main PI-institute and we are indebted to ESA for their courage in embarking on the Mars Express program, the first ESA mission to the red planet.

ASPERA-3 Team

R. A. Frahm, J. D. Winningham, J. R. Sharber, *SwRI, San Antonio, USA*
A. J. Coates, D. R. Linder, D. O. Kataria, *Mullard Space Science Laboratory, UCL, UK*
R. Lundin, H. Anderson, S. Barabash, M. Holmstrom, M. Yamauchi, *Swedish Institute of Space Physics, Sweden*
E. Kallio, H. Koskinen, *Finnish Meteorological Institute, Helsinki, Finland*
J. Kozyra, *Space Physics Research Laboratory, U. Michigan, Ann Arbor, USA*
J. Luhmann, *University of California Berkeley, USA*
E. Roelof, D. Williams, *JHU-APL, Laurel, USA*
C.C. Curtis, K. C. Hsieh, B. R. Sandel, *University of Arizona, Tucson, USA*
J. A. Sauvaud, A. Federov, *Centre d'Etude Spatiale des Rayonnements, France*
S. McKenna-Lawlor, *Space Technology Ltd, Maynooth, Ireland*
S. Orsini, R. Cerulli-Irelli, *Institute di Fisica dello Spazio Interplantari, Italy*
P. Bochsler, P. Wurz, *University of Bern, Bern Switzerland*
K. Azamura, *ISAS, Japan*
M. Grande, *Rutherford Appleton Laboratory, Oxfordshire, UK*
N. Krupp, J. Woch, M. Fraenz, *Max-Planck-Institut fur Aeronomie, Germany*

References

Barabash, S., R. Lundin, H. Andersson, J. Gimholt, M. Holmström, O. Norberg, M. Yamauchi, K. Asamura, A. J. Coates, D. R. Linder, D. O. Kataria, C. C. Curtis, K. C. Hsieh, B. R. Sandel, A. Fedorov, A. Grigoriev, E. Budnik, M. Grande, M. Carter, D. H. Reading, H. Koskinen, E. Kallio, P. Riihela, T. Säles, J. Kozyra, N. Krupp, S. Livi, J. Woch, J. Luhmann, S. McKenna-Lawlor, S. Orsini, R. Cerulli-Irelli, A. Mura, A. Milillo, E. Roelof, D. Williams, J.-A. Sauvaud, J.-J. Thocaven, D. Winningham, R. Frahm, J. Scherrer, J. Sharber, P. Wurz, and P. Bochsler, "The Analyzer of Space Plasmas and Energetic Atoms (ASPERA-3) for the Mars Express Mission," EGS XXV General Assembly, Nice, France, April 2000. (http://www.aspera-3.org/ASPERA_paper_new.pdf)

Barabash, S., R. Lundin, H. Andersson, J. Gimholt, M. Holmström, O. Norberg, M. Yamauchi, K. Asamura, A. J. Coates, D. R. Linder, D. O. Kataria, C. C. Curtis, K. C. Hsieh, B. R. Sandel, A. Fedorov, A. Grigoriev, E. Budnik, M. Grande, M. Carter, D. H. Reading, H. Koskinen, E. Kallio, P. Riihela, T. Säles, J. Kozyra, N. Krupp, S. Livi, J. Woch, J. Luhmann, S. McKenna-Lawlor, S. Orsini, R. Cerulli-Irelli, A. Mura, A. Milillo, E. Roelof, D. Williams, J.-A. Sauvaud, J.-J. Thocaven, D. Winningham, R. Frahm, J. Scherrer, J. Sharber, P. Wurz, and P. Bochsler, "ASPERA-3: Analyser of Space Plasmas and Energetic Ions for the Mars Express," in Mars Express: The Scientific Payload, eds. A. Wilson and A. Chicarro, European Space Agency special report SP-1240, European Space Agency Research and Scientific Support, European Space Research and Technology Centre, Noordwijk, The Netherlands, 121-139, August 2004.

Fox, J. L., and A. Dalgarno, "Ionization, Luminosity, and Heating of the Upper Atmosphere of Mars," Journal of Geophysical Research, 84, 7315-7333, 1979.

Mantas, G. P., and W. B. Hanson, "Photoelectron Fluxes in the Martian Ionosphere," Journal of Geophysical Research, 84, 369-385, 1979.

Mitchell, D. L., R. P. Lin, C. Mazelle, H. Rème, P. A. Cloutier, J. E. P. Connerney, M. H. Acuña, and N. F. Ness, "Probing Mars' crustal magnetic field and ionosphere with the MGS Electron Reflectometer," Journal of Geophysical Research, 106, 23419-23427, 2001.

PO0094